

Nuclear Fusion Inside Dark Matter

Javier F. Acevedo,¹ Joseph Bramante,^{1,2} and Alan Goodman¹

¹*The McDonald Institute and Department of Physics, Engineering Physics, and Astronomy, Queen's University, Kingston, Ontario, K7L 2S8, Canada*

²*Perimeter Institute for Theoretical Physics, Waterloo, Ontario, N2L 2Y5, Canada*

A new dynamic is identified between dark matter and nuclei. Nuclei accelerated to MeV energies by the internal potential of composite dark matter can undergo nuclear fusion. This effect arises in simple models of composite dark matter made of heavy fermions bound by a light scalar field. Cosmologies and detection prospects are explored for composites that catalyze nuclear reactions in underground detectors and stars, including bremsstrahlung radiation from nuclei scattering against electrons in hot plasma formed in the composite interior. If discovered and collected, this kind of composite dark matter could in principle serve as a ready-made, compact nuclear fusion generator.

I. INTRODUCTION

The presence of dark matter has become manifest through galactic dynamics, the lensing of light, and temperature fluctuations in the cosmic microwave background. But setting aside these gravitational signifiers, little is known about dark matter despite extensive laboratory and astrophysical efforts. It is a high priority of modern science to uncover dark matter, identify its mass and couplings, and determine what influence it may have on other particles that compose the known universe.

In the past decade theorists have enunciated how a certain variety of dark matter could bear a striking resemblance to known matter. Atoms, nuclei, and nucleons, which comprise the bulk of known particles, are all built from fundamental fermions – electrons, protons, quarks – bound together by photons and gluons into composite states. Similarly, dark matter could also be comprised of many particles bound together in a composite state [1–14]. One simple composite dark matter model consists of fermions (X) bound by a new attractive force provided by a massive scalar field (φ) [15–21]. If this force is strong enough, then in the early universe large dark matter states would be built from successive fusion of X particles into increasingly massive states, in a process similar to big bang nucleosynthesis (BBN). In the absence of the repulsive Coulomb force between protons in Standard Model nuclei, these dark composites can become extremely massive after accumulating oodles of X particles. As we will see in this work, if X has a TeV–EeV mass, this can imply dark matter composite masses ranging from a few micrograms to thousands of tons.

We have found that such large dark matter (DM) composites imply novel dynamical interactions with Standard Model nuclei. In this paper we present these newly identified dynamics. Large composite dark matter can cause Standard Model (SM) nuclei to accelerate, radiate, and fuse in the composite interior, as shown in Fig. 1. These dynamics occur because the scalar field binding X particles together can have an extremely high potential $\langle\varphi\rangle$ inside the dark matter composite. Under the influence of this potential, SM nuclei are accelerated to energies $\Delta E \sim g_n \langle\varphi\rangle \sim \text{MeV}$, sufficient to initiate nuclear fu-

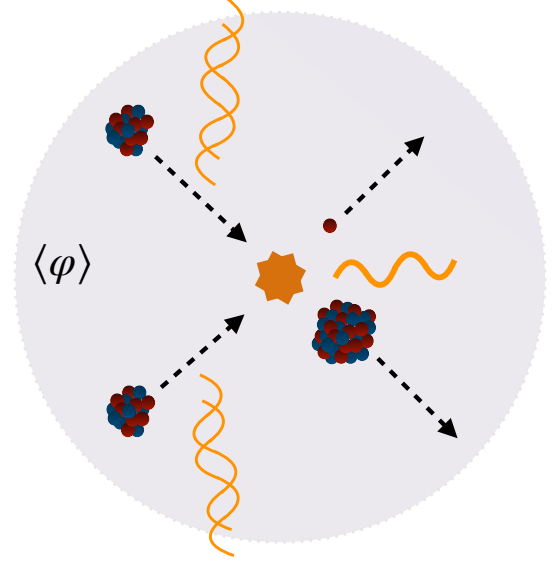


Figure 1. Schematic of nuclei accelerated by the potential $\langle\varphi\rangle$ inside a dark matter composite, resulting in ionization, bremsstrahlung radiation, and thermonuclear fusion. A typical fusion reaction is shown where two oxygen combine to make phosphorous, a proton, and ~ 7.7 MeV excess energy.

sion and radiation from high energy collisions, even for a miniscule Yukawa coupling g_n between φ and nucleons. This implies new signatures and even potential uses for composite dark matter, including nuclear fusion and bremsstrahlung radiation as unique signatures in particle detectors, nuclear reactions in stars and planets, and speculatively the use of composites as compact fusion reactors. In addition, we find that the largest fusion-capable composites would make white dwarfs explode.

II. HEAVY COMPOSITE COSMOLOGY

We begin with the cosmology of very large composites, formed from heavy asymmetric fermions with masses ranging up to an EeV. As we will see, dark composites formed from such heavy fermions can have large inter-

nal potentials that accelerate Standard Model nuclei to fusion temperatures. The cosmology of up to 10^{10} GeV mass asymmetric dark matter, motivated by high scale baryogenesis mechanisms like Affleck-Dine [22, 23], has been detailed in [24]. In asymmetric dark matter models [25, 26], an initial dark sector particle asymmetry sets the dark matter relic abundance, and typically dark matter freeze-out annihilation eliminates most of the symmetric dark matter abundance, *i.e.* $X + \bar{X} \rightarrow \text{SM}$, leaving behind a residual asymmetric abundance of X particles. For a heavy asymmetric dark matter scenario [24], the abundance of dark fermions is subsequently depleted (along with the baryon abundance) by *e.g.* the decay of a field some time after freeze-out. The amount the asymmetric dark matter (and baryon) abundance is depleted by this decay is given by $\Omega_{DM}^{dep} = \Omega_{DM}\zeta$, where $\zeta = s_{before}/s_{after}$ is the ratio of entropy density in the universe before and after the field decays [24]. In the models that follow, we will assume that dark fermions freeze-out to an initial abundance that is later diluted through the decay of a metastable field [23, 27–31], or a phase transition/second phase of inflation [32–37]. This means that right after its freeze-out, dark matter’s abundance will be larger by a factor of ζ^{-1} , relative to a cosmology without subsequent depletion. We will see that this relative overabundance of X after freeze-out leads to the formation of rather large DM composites.

Asymmetric DM composites made of sub-TeV mass fermions have been studied at length in [15–21]. Here we consider heavier fermions. The Lagrangian,

$$\mathcal{L} = \frac{1}{2}(\partial\varphi)^2 + \bar{X}(i\gamma^\mu\partial_\mu - m_X)X + g_X\bar{X}\varphi X - \frac{1}{2}m_\varphi^2\varphi^2 + g_n\bar{n}\varphi n + \mathcal{L}_{SM}, \quad (1)$$

includes the scalar φ which provides an attractive force that binds together X fermions. The second to last term couples φ to SM nucleons n , and \mathcal{L}_{SM} is the SM Lagrangian. Once enough X particles are bound together, fermionic composites will reach a saturation point after the composite radius exceeds $R_X \gtrsim m_\varphi^{-1}$, at which point the interior density becomes approximately constant, $\rho_c = \bar{m}_X^4/3\pi^2$, where \bar{m}_X is the constituent mass, *i.e.* the effective mass of X inside the composite [19, 20]. For the cosmological formation we consider hereafter, composites are saturated well before they finish forming, *c.f.* Eq. (2). The constituent mass for a saturated composite is given by $\bar{m}_X \simeq m_X - E_X$, where E_X is the binding energy per X . In terms of bare masses and couplings, in a saturated composite $\bar{m}_X \simeq [3\pi m_X^2 m_\varphi^2 / (2\alpha_X)]^{1/4}$, where the $\varphi - X$ coupling constant is $\alpha_X \equiv g_X^2/4\pi$. For parameters we consider, the binding energy is close to the unbound X mass, $E_X \sim m_X$, and so $\bar{m}_X \ll m_X$. This means the composite state of X particles has a total mass $M_X \equiv N\bar{m}_X$, which is much less than the mass of unbound X particles, Nm_X . As a consequence, after the composite is assembled, the mass density of dark matter in the universe decreases by a factor \bar{m}_X/m_X , where the mass loss is accounted for by the emission of φ radiation.

Fermion composites will begin to assemble in the early universe by forming two-fermion bound states, where binding will occur so long as $\alpha_X^2 m_X \gtrsim m_\varphi$ and $\alpha_X \gtrsim 0.3 (m_X/10^7 \text{ GeV})^{2/5} (\zeta/10^{-6})^{1/5}$ [15]. After two-fermion states form, composites will build up through processes like $X_N + X_N \rightarrow X_{2N} + \varphi$, where X_N is a bound state formed from N fermions. At the temperature of composite assembly T_{ca} , an estimate for the number of constituent particles in a typical composite can be obtained by comparing the X_N interaction rate to the Hubble rate [17, 20], $n_{X_N}\sigma_{X_N}v_{X_N}/H \sim 1$. Re-expressing this in terms of the X number density $n_X = n_{X_N}/N$, the X composite cross-section $\sigma_X = \sigma_{X_N}/N^{2/3}$ (where R_X scales as $N^{1/3}$ in the saturation regime), and the X velocity $v_{X_N} = v_X/N^{1/2}$, we arrive at an expression for the number of X particles in a typical composite,

$$N_c = \left(\frac{2n_X\sigma_X v_X}{3H}\right)^{6/5} = \left(\frac{20\sqrt{g_{ca}^*}T_r T_{ca}^{3/2} M_{pl}}{\bar{m}_X^{7/2}\zeta}\right)^{6/5} \quad (2)$$

$$\simeq 10^{27} \left(\frac{g_{ca}^*}{10^2}\right)^{3/5} \left(\frac{T_{ca}}{10^5 \text{ GeV}}\right)^{9/5} \left(\frac{5 \text{ GeV}}{\bar{m}_X}\right)^{21/5} \left(\frac{10^{-6}}{\zeta}\right)^{6/5},$$

where in the first equality we have included a factor of $2/3$ appropriate for composite assembly in a radiation-dominated universe [20], in the second equality we have used a composite cross-section $\sigma_X = 4\pi R_c^2$ with $R_c \equiv (3\rho_c/4\pi)^{1/3} = (9\pi/4)^{1/3}/\bar{m}_X$, a velocity $v_X = \sqrt{T/\bar{m}_X}$, the Friedmann relation is $3H^2 M_{pl}^2 = g^*\pi^2 T^4/30$ for Planck mass M_{pl} and temperature T , and we estimate the X density at the time of composite assembly as $n_X = g_{ca}^*\pi^2 T_{ca}^3/(30\zeta\bar{m}_X)$, where $T_r \simeq 0.8 \text{ eV}$ is the temperature at matter-radiation equality. For $m_X \gg \bar{m}_X$, the binding energy of these composites is $E_X \sim m_X$, and composite assembly will finish around the temperature of X freeze-out, $T_{ca} \sim m_X/10$.

A few more facets of heavy composite cosmology are worth emphasizing. First, because the constituent mass $\bar{m}_X \ll m_X$ determines the final density of DM, heavy asymmetric DM composites can account for the baryon-DM density coincidence: the present-day DM density approximately matches the baryon density, $\Omega_{DM}/\Omega_B \sim 5$. For asymmetric DM, this coincidence can be explained by having a single particle asymmetry that determines both the baryon and DM relic abundances. While a naive prediction for the constituent DM mass relative to the baryon mass is then $\bar{m}_X \sim 5m_b \sim 5 \text{ GeV}$, in the case that heavy asymmetric DM freezes out before the electroweak phase transition, electroweak sphalerons can dilute baryon number, leading to a looser prediction $\bar{m}_X \sim 1 - 1000 \text{ GeV}$ [25]. Second, as previously discussed, in an asymmetric DM cosmology the symmetric DM component ($X\bar{X}$) is depleted via annihilation. In the case of the heavy DM detailed above, $X\bar{X}$ annihilation to φ will deplete $X\bar{X}$ to a sub-DM relic density, if the annihilation cross-section $\sigma_a v \simeq 3\pi\alpha_X^2/(8m_X^2) \gtrsim 10^{-36} \text{ cm}^2 \times \zeta$ [24], which corresponds to $\alpha_X \gtrsim 0.3 (m_X/10^7 \text{ GeV}) (\zeta/10^{-6})^{1/2}$, although this

restriction weakens if $X\bar{X}$ are depleted by additional annihilation channels or other mechanisms.

III. NUCLEAR ACCELERATION, RADIATION, AND FUSION IN COMPOSITE DM

Substantial energy can be released by nuclei accelerated inside large DM composites, both through fusion and bremsstrahlung processes. With the structure and cosmology of heavy composites previously laid out, we now turn to nuclear acceleration, radiation, and fusion inside large composites. We begin with the potential inside a saturated composite $\langle\varphi\rangle \simeq \frac{m_X}{g_X}$, obtained by requiring the composite's internal potential (1) is minimized at equilibrium. Boundary conditions require that outside the composite the potential decays as

$$\varphi(r) = \langle\varphi\rangle e^{-m_\varphi(r-R_X)} \left(\frac{R_X}{r}\right). \quad (3)$$

Acceleration. Nuclei with A nucleons will have their momentum p boosted to p' as they enter the composite, according to $p^2 + m_N^2 = p'^2 + (m_N - V_n)^2$, where $V_n = Ag_n\langle\varphi\rangle = Ag_n m_X/g_X$. In the limit $V_n \ll m_N$, the second term can be expanded yielding $p^2 - p'^2 = 2m_N V_n$. Nuclei will accelerate over a time determined by the field gradient at the composite boundary and the velocity v_X at which the composite moves, *cf.* Eq. (3), $\tau_{\text{accel}} \simeq (m_\varphi v_X)^{-1} (1 + 2V_n/m_N v_X^2)^{-1/2}$.

Ionization. For parameters in Fig. 2 saturated composites crossing terrestrial material at speeds $v_X \simeq 10^{-3}$ will accelerate nuclei on a timescale $\tau_{\text{accel}} \lesssim 10^{-18}$ s due to the sharp gradient of the potential. This timescale is shorter than both the electron orbital period $(10 \text{ eV})^{-1} \simeq 10^{-17}$ s and $a_0/v_N \simeq 10^{-17}$ s $(v_N/10^{-2})^{-1}$ where v_N is the nucleus final speed and a_0 is the Bohr radius. Such a perturbation is then non-adiabatic, *i.e.* electrons do not respond to the sudden nuclear motion in a similar timescale, resulting in excitation or ionization [40, 41], the so-called Migdal effect which has been recently considered to extend the sensitivity of direct detection experiments [42–48]. In particular, numerical results from [42] indicate that the probability of outer-shell electron ionization for C and O atoms, the most abundant elements in IceCube and SNO+, is of order $f_e \simeq 10^{-2} - 10^{-1}$ for the nuclear kinetic energies considered here, with the probability peak located at ionized electron energies $\sim 1 - 10$ eV. Hence after this impulsive motion, a sizeable fraction of atoms are partially ionized. However, further considerations indicate the atoms will be fully ionized. The atoms accelerated to $T \simeq 100 \text{ eV} - 1 \text{ MeV}$ inside the composite, will scatter with ionized free electrons, resulting in further ionization. The cross-section for ionizing atomic oxygen or carbon is $\sigma_i \sim 10^{-16} - 10^{-17} \text{ cm}^2$ in the energy range of interest [49]. Ionization by electron-atom collisions will occur on a timescale given by $(f_e n_e v_N \sigma_i)^{-1} \lesssim 10^{-15}$ s, where v_N is the atom velocity and $n_e \simeq 10^{23} \text{ cm}^{-3}$ is the electron number den-

sity. This timescale is shorter than the composite crossing time $(2R_X/v_X) \gtrsim 10^{-15} \text{ s}$ $(R_X/\text{nm})(v_X/10^{-3})^{-1}$, so long as composites are larger than a nm, and becomes even shorter as more electrons are ionized and $f_e \sim 1$. Hence atoms are fully ionized in the detection regions shown in Fig. 2. These estimates agree with [50], which finds order one ionization fractions for carbon and oxygen plasmas at $T \gtrsim 100 \text{ eV}$ and density $\sim 1 \text{ g cm}^{-3}$.

Radiation. The ion-electron plasma will have a photon opacity dominated by free-electron scattering, with a photon mean free path $(n_e \sigma_T)^{-1} \simeq 5 \text{ cm} \gg R_X$, where $\sigma_T \sim 10^{-24} \text{ cm}^2$ is the Thompson cross-section for electrons. Therefore, radiation never equilibrates with the plasma and we do not expect blackbody radiation. Instead, we expect thermal electron-ion bremsstrahlung, which has specific emissivity at frequency ω (see *e.g.* [51]) $j_\omega = (16\pi e^6 n_e^2 / 3\sqrt{3} m_e^2) (2m_e / \pi T)^{1/2} \exp(-\omega/T)$, for electron mass m_e and fine structure constant $e^2/4\pi$. Since in Fig. 2 we require $T \gtrsim 100 \text{ eV}$, there is emission of ionizing radiation. The integrated emissivity over volume and frequency yields a radiated energy rate

$$\begin{aligned} \dot{E}_{\text{brem}} &= \frac{64\pi^2 e^6}{9\sqrt{3} m_e^2} \left(\frac{2m_e T}{\pi}\right)^{\frac{1}{2}} n_e^2 R_X^3 \\ &\simeq 10^{10} \text{ GeV s}^{-1} \left(\frac{g_X}{1}\right)^{-\frac{1}{2}} \left(\frac{g_n}{10^{-10}}\right)^{\frac{1}{2}} \left(\frac{m_X}{\text{TeV}}\right)^{\frac{1}{2}} \left(\frac{R_X}{\text{nm}}\right)^3. \end{aligned} \quad (4)$$

At temperatures $T \sim 100 \text{ keV} - 1 \text{ MeV}$, we also expect a fraction of the ions to undergo thermonuclear fusion. In particular, we consider here the thermonuclear ^{16}O burning rate tabulated in [52], since this is the most abundant isotope in the terrestrial crust and mantle [53–58].

Detection. The large composites we have uncovered cannot be found by traditional dark matter experiments, which are flux limited to $M_X \lesssim 10^{19} \text{ GeV}$ [9, 59]. However, the copious energy released by fusion-capable composites make them observable at larger neutrino experiments like IceCube, Super-K, and large volume scintillators (LVS) like SNO+, Borexino, and JUNO; their enormity extends the M_X mass reach to $3 \times 10^{25} \text{ GeV}$ in the case of IceCube (assuming 5 yrs and a km^2 detection area). To conservatively establish the sensitivity of IceCube and LVS to a flood of $\gtrsim \text{eV}$ photons emitted from transiting composites, in Fig. 2 we require trigger threshold energy depositions of $\sim 10 \text{ TeV}$ and 1 MeV per 100 ns respectively, which are an order of magnitude above the TeV [60] and 100 keV [61, 62] per 100 ns design thresholds of these experiments (this still underestimates IceCube's sensitivity, since our requirement implies $\gtrsim 100 \text{ PeV}$ radiated in a transit through IceCube). Comparing this to Eq. (4), we find that nucleon couplings as small as $g_n \sim 10^{-14}$ at IceCube and $g_n \sim 10^{-12}$ at LVS can be detected for regions marked in Fig. 2. We also show where ^{16}O fusion reactions occur at IceCube as a single composite crosses it, using the ^{16}O burning rate in [52]. In this case, there will be additional gamma rays and byproducts with $\sim \text{MeV}$ energies, *e.g.* $^{32,31}\text{S}$, ^{32}P , ^{28}Si , ^{24}Mg as well as p, n and α 's [52].

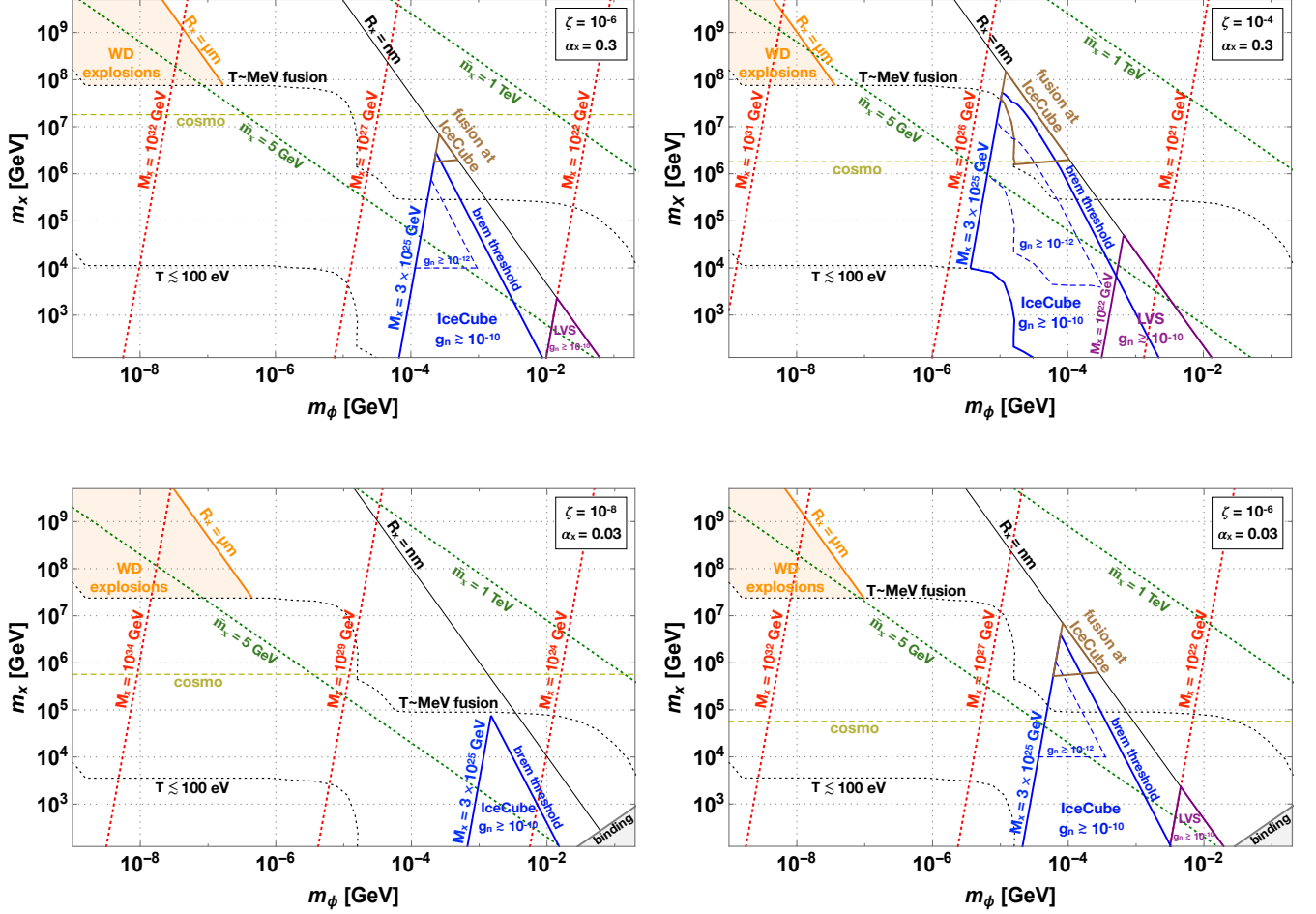


Figure 2. Heavy asymmetric composites that cause nuclei to radiate and fuse in their interiors, for fermion mass m_X , scalar mass m_φ , and $\varphi-X$ coupling α_X . The total mass of the composites $M_X = N_c \bar{m}_X$ is shown with red dashed lines, determined by composite assembly after DM freeze-out, followed by a process that dilutes relic abundances by ζ , cf. Eq. (2). The baryon and DM densities could arise from a common asymmetry for $\bar{m}_X \approx 5 - 1000$ GeV. Blue and purple regions show what composites can be discovered via bremsstrahlung at IceCube and scintillator (LVS) experiments, for φ -nucleon couplings $g_n \geq 10^{-10}$ and $g_n \geq 10^{-12}$ as indicated (one plot omits the $g_n \geq 10^{-12}$ region for clarity). For detection we require $R_X \gtrsim \text{nm}$, so composites contain $\gtrsim 10$ atoms at solid Earth densities. Above the dotted line labelled “T~MeV fusion,” the maximum g_n allowed by stellar and fifth force bounds [38, 39], permits nuclei to be accelerated to MeV temperatures (the $T < 100$ eV line is obtained the same way). In the tan wedges, DM can cause nuclei to fuse at IceCube. The heaviest fusion-capable composites can be excluded by old white dwarfs not exploding. Below the yellow dashed line labelled “cosmo,” the composite assembly cosmology detailed in the text is satisfied for α_X, ζ values. A strong binding condition $\alpha_X^2 m_X \gtrsim m_\varphi$ [16] limits the bottom panels.

Capture on Earth and lack of X-nuclear scattering. Thus far we have not mentioned nuclear scattering against X fermions in composites. Compared to Eq. (4), composite energy loss from X -nuclear scattering will be negligible, in part because the fermi momentum of X is large, $p_{fX} \sim \bar{m}_X$. Accounting for nuclear scattering with degenerate fermions [63–65], the scattering energy loss for $m_N \ll \bar{m}_X$ is $\dot{E}_{X-N} \approx A^2 g_n^2 g_X^2 m_N^5 p_{fX}^{-3} v_X^8$ and for $\bar{m}_X \ll m_N$ is $\dot{E}_{X-N} \approx A^2 g_n^2 g_X^2 p_{fX}^2 v_X^2$, which are tiny compared to bremsstrahlung in Fig. 2. On the other hand, energy loss in the form of radiation, cf. Eq. (4), could result in stopping and capture of composites as

they cross the Earth. A composite with an initial velocity v_X will travel through the Earth’s mantle a distance $L_{\text{cap}} \simeq 2 \text{ km} (m_X/\text{TeV})^{3/2} (10^{-10}/g_n)^{1/2} (g_X/1)^{-3/2} \times (v_X/200 \text{ km s}^{-1})^3 (m_\varphi/10 \text{ keV})^2$ before being slowed below Earth’s escape velocity, where we have computed this distance considering the most abundant isotope ^{16}O and using elemental/density profiles from [66, 67] (see also [53–58]). Earth’s composite capture rate can be found using the method described in [67]. Further implications of composite capture will be studied elsewhere [65].

WD explosions. The transit of a large composite through a white dwarf (WD) can catalyze nuclear

fusion reactions leading to a thermonuclear runaway and Type-Ia supernova explosion, similar to [68–73], although in this case fusion is initiated by nuclei accelerated inside the composite. For WD ignition conditions, we use the results of [74], where a set of critical temperatures and trigger masses are numerically computed for different white dwarf compositions. As a benchmark value, we require a critical temperature $T_{\text{crit}} \simeq 1$ MeV for a pure ^{12}C white dwarf. First, we note that as they pass through a white dwarf, composites can lose a small amount of kinetic energy to heat dissipation in the form of conduction and radiation. However, composites bounded by WDs in Fig. 2 are so massive that a negligible fraction of their kinetic energy is lost to this dissipative effect. Heat conduction out of the composite is dominated by relativistic white dwarf electrons, with a rate $\dot{Q}_{\text{cond}} \simeq 4\pi^2 T_X^4 R_X / 15\kappa_c \rho_* \approx 10^{27} \text{ GeV s}^{-1} (\rho_*/10^9 \text{ g cm}^{-3})^{4/15} (R_X/\mu\text{m})$, where $\kappa_c \simeq 10^{-9} \text{ cm}^2/\text{g} (T_*/10^7 \text{ K})^{2.8} (10^9 \text{ g cm}^{-3}/\rho)^{1.6}$ is the conductive opacity of the relativistic white dwarf electrons [75]. Composite radiation, on the other hand, is $\dot{Q}_{\text{rad}} = 4\pi R_X^2 \nabla(\sigma T^4)/\kappa_r \rho_* \simeq 16\pi R_X^2 \sigma T^4 m_\varphi/\kappa_r \rho_* \simeq 10^{22} \text{ GeV s}^{-1} (R_X/\mu\text{m})^2 (m_\varphi/\text{keV})$, where $\kappa_r \simeq 10^{24} \text{ cm}^2 \text{ g}^{-1} (T_*/10^7 \text{ K})^{-7/2} (\rho_*/10^9 \text{ g cm}^{-3})$ is the radiative opacity of the white dwarf medium [76]. Here we assume a blackbody energy density since the stellar material is highly opaque to photons.

The rate of carbon fusion in dense WD matter is $\dot{R}_{th} \simeq 10^{42} \text{ cm}^{-3} \text{ s}^{-1} (\rho_*/10^9 \text{ g cm}^{-3})^2$ at $T_{\text{crit}} \simeq 1$ MeV, with an average energy release rate $Q \simeq +3$ MeV per reaction [77]. This yields a nuclear energy release rate $\dot{Q}_{\text{fus}} \simeq 4\pi Q \dot{R}_{th} R_X^3/3 \gtrsim 10^{28} \text{ GeV s}^{-1} (R_X/\mu\text{m})^3$. Therefore, for composites with radii $R_X \gtrsim \mu\text{m}$, the heat release from nuclear fusion greatly exceeds conductive and radiative losses, setting the conditions for a sustained thermonuclear runaway. We remark that stellar masses contained within radii $\gtrsim \mu\text{m}$ are $\gtrsim 10^{-3} \text{ g}$, which are in agreement with the minimum trigger masses outlined in [74]. Fig. 2 shows the region where $V_n \sim \text{MeV}$ composites ignite a WD by simply passing through. Since one encounter would occur for composite masses $M_X \lesssim 10^{42} \text{ GeV}$ in a $\sim \text{Gyr}$ timescale, the survival of *e.g.* WD J160420.40 [71] implies constraints on nucleon couplings $g_n \lesssim 10^{-12} (m_X/10^8 \text{ GeV})^{-1}$ in that region.

BBN. It is natural to wonder whether BBN may constrain fusion-capable composites through overproduction or disintegration of isotopes. An extensive analysis of fusion-capable DM composites on primordial abundances using relevant reaction rates (*e.g.* [78–80]) will be the subject of future work. Here we remark that in the IceCube and LVS detection regions shown in Fig. 2, early universe composites seem unlikely to alter standard BBN abundance predictions. Constraints on g_n imply that even for the maximum coupling allowed, composites

will not change the temperature of the primordial plasma until redshift $z_X \lesssim 10^5 (A/1)(g_n/10^{-10})(m_X/\text{TeV})$. However, by this redshift the baryon density will be significantly diluted according to $\Omega_b \rho_c (1+z_X)^3$. The average number of baryons inside composites will then be $4\pi \Omega_b \rho_c (1+z_X)^3 R_X^3/3m_b \simeq 10^{-11} (m_X/\text{TeV})^3 (g_n/10^{-10})^3 (R_X/\text{nm})^3$ where m_b is the baryon mass. Comparing this to Fig. 2, parameter space where large neutrino experiments have sensitivity, corresponds to composite sizes too small to have more than one baryon per composite, by the time a baryon inside a composite would be substantially accelerated in the early universe. Similar estimates using Eq. (4) and preceding text indicate that detectable fusion-capable composites do not observably alter the baryon-to-photon ratio after BBN, nor the ionization fraction after recombination.

IV. CONCLUSIONS

We have studied the cosmology and detection of heavy composite DM that internally accelerates nuclei, resulting in copious collisional radiation and nuclear fusion. Prospects have been explored for detection of fusion-capable composites at IceCube and liquid scintillator experiments. There are many aspects of Standard Model particle acceleration in DM composites that remain. While here we considered composites that accelerate nuclei to MeV energies, if this were increased to relativistic energies, this would cause repulsive composite-SM scattering processes [81]. For smaller than 100 eV acceleration energies, the Migdal effect and SM-SM collisional ionization should permit dark matter experiments to search for rather weakly-coupled composites. Given that asymmetric composites are often associated with SM asymmetries, similar acceleration effects should be explored for composites coupled to the SM through vector fields, and especially fields that couple to leptons, baryons, or a combination of these. Finally, it would be interesting to study whether fusion-capable composites could detectably alter isotopic abundances in the Earth over geological time periods. We leave these and other inquests into accelerative dark matter to future work.

ACKNOWLEDGEMENTS

We thank Nirmal Raj for discussions and comments on the manuscript. The work of JA, JB, AG is supported by the Natural Sciences and Engineering Research Council of Canada (NSERC). Research at Perimeter Institute is supported in part by the Government of Canada through the Department of Innovation, Science and Economic Development Canada and by the Province of Ontario through the Ministry of Colleges and Universities.

-
- [1] S. Nussinov, “Technoc cosmology: could a technibaryon excess provide a ‘natural’ missing mass candidate?” *Phys. Lett. B* **165**, 55–58 (1985).
- [2] John Bagnasco, Michael Dine, and Scott D. Thomas, “Detecting technibaryon dark matter,” *Phys. Lett. B* **320**, 99–104 (1994), [arXiv:hep-ph/9310290](#).
- [3] Daniele S. M. Alves, Siavosh R. Behbahani, Philip Schuster, and Jay G. Wacker, “Composite Inelastic Dark Matter,” *Phys. Lett. B* **692**, 323–326 (2010), [arXiv:0903.3945 \[hep-ph\]](#).
- [4] Graham D. Kribs, Tuhin S. Roy, John Terning, and Kathryn M. Zurek, “Quirky Composite Dark Matter,” *Phys. Rev. D* **81**, 095001 (2010), [arXiv:0909.2034 \[hep-ph\]](#).
- [5] Hyun Min Lee, Myeonghun Park, and Veronica Sanz, “Gravity-mediated (or Composite) Dark Matter,” *Eur. Phys. J. C* **74**, 2715 (2014), [arXiv:1306.4107 \[hep-ph\]](#).
- [6] Gordan Krnjaic and Kris Sigurdson, “Big Bang Dark-leosynthesis,” *Phys. Lett. B* **751**, 464–468 (2015), [arXiv:1406.1171 \[hep-ph\]](#).
- [7] William Detmold, Matthew McCullough, and Andrew Pochinsky, “Dark Nuclei I: Cosmology and Indirect Detection,” *Phys. Rev. D* **90**, 115013 (2014), [arXiv:1406.2276 \[hep-ph\]](#).
- [8] David M. Jacobs, Glenn D. Starkman, and Bryan W. Lynn, “Macro Dark Matter,” *Mon. Not. Roy. Astron. Soc.* **450**, 3418–3430 (2015), [arXiv:1410.2236 \[astro-ph.CO\]](#).
- [9] Joseph Bramante, Benjamin Broerman, Jason Kumar, Rafael F. Lang, Maxim Pospelov, and Nirmal Raj, “Foraging for dark matter in large volume liquid scintillator neutrino detectors with multiscatter events,” *Phys. Rev. D* **99**, 083010 (2019), [arXiv:1812.09325 \[hep-ph\]](#).
- [10] Masahiro Ibe, Ayuki Kamada, Shin Kobayashi, and Wakutaka Nakano, “Composite Asymmetric Dark Matter with a Dark Photon Portal,” *JHEP* **11**, 203 (2018), [arXiv:1805.06876 \[hep-ph\]](#).
- [11] Ahmet Coskuner, Dorota M. Grabowska, Simon Knapen, and Kathryn M. Zurek, “Direct Detection of Bound States of Asymmetric Dark Matter,” *Phys. Rev. D* **100**, 035025 (2019), [arXiv:1812.07573 \[hep-ph\]](#).
- [12] Yang Bai, Andrew J. Long, and Sida Lu, “Dark Quark Nuggets,” *Phys. Rev. D* **99**, 055047 (2019), [arXiv:1810.04360 \[hep-ph\]](#).
- [13] Yang Bai and Joshua Berger, “Nucleus Capture by Macroscopic Dark Matter,” *JHEP* **05**, 160 (2020), [arXiv:1912.02813 \[hep-ph\]](#).
- [14] Joseph Bramante, Jason Kumar, and Nirmal Raj, “Dark matter astrometry at underground detectors with multiscatter events,” *Phys. Rev. D* **100**, 123016 (2019), [arXiv:1910.05380 \[hep-ph\]](#).
- [15] Mark B. Wise and Yue Zhang, “Stable Bound States of Asymmetric Dark Matter,” *Phys. Rev. D* **90**, 055030 (2014), [Erratum: *Phys. Rev. D* **91**, 039907 (2015)], [arXiv:1407.4121 \[hep-ph\]](#).
- [16] Mark B. Wise and Yue Zhang, “Yukawa Bound States of a Large Number of Fermions,” *JHEP* **02**, 023 (2015), [Erratum: *JHEP* **10**, 165 (2015)], [arXiv:1411.1772 \[hep-ph\]](#).
- [17] Edward Hardy, Robert Lasenby, John March-Russell, and Stephen M. West, “Big Bang Synthesis of Nuclear Dark Matter,” *JHEP* **06**, 011 (2015), [arXiv:1411.3739 \[hep-ph\]](#).
- [18] Edward Hardy, Robert Lasenby, John March-Russell, and Stephen M. West, “Signatures of Large Composite Dark Matter States,” *JHEP* **07**, 133 (2015), [arXiv:1504.05419 \[hep-ph\]](#).
- [19] Moira I. Gresham, Hou Keong Lou, and Kathryn M. Zurek, “Nuclear Structure of Bound States of Asymmetric Dark Matter,” *Phys. Rev. D* **96**, 096012 (2017), [arXiv:1707.02313 \[hep-ph\]](#).
- [20] Moira I. Gresham, Hou Keong Lou, and Kathryn M. Zurek, “Early Universe synthesis of asymmetric dark matter nuggets,” *Phys. Rev. D* **97**, 036003 (2018), [arXiv:1707.02316 \[hep-ph\]](#).
- [21] Moira I. Gresham, Hou Keong Lou, and Kathryn M. Zurek, “Astrophysical Signatures of Asymmetric Dark Matter Bound States,” *Phys. Rev. D* **98**, 096001 (2018), [arXiv:1805.04512 \[hep-ph\]](#).
- [22] Ian Affleck and Michael Dine, “A New Mechanism for Baryogenesis,” *Nucl. Phys. B* **249**, 361–380 (1985).
- [23] Michael Dine, Lisa Randall, and Scott D. Thomas, “Baryogenesis from flat directions of the supersymmetric standard model,” *Nucl. Phys. B* **458**, 291–326 (1996), [arXiv:hep-ph/9507453 \[hep-ph\]](#).
- [24] Joseph Bramante and James Unwin, “Superheavy Thermal Dark Matter and Primordial Asymmetries,” *JHEP* **02**, 119 (2017), [arXiv:1701.05859 \[hep-ph\]](#).
- [25] Kathryn M. Zurek, “Asymmetric Dark Matter: Theories, Signatures, and Constraints,” *Phys. Rept.* **537**, 91–121 (2014), [arXiv:1308.0338 \[hep-ph\]](#).
- [26] Kalliopi Petraki and Raymond R. Volkas, “Review of asymmetric dark matter,” *Int. J. Mod. Phys. A* **28**, 1330028 (2013), [arXiv:1305.4939 \[hep-ph\]](#).
- [27] Tom Banks, David B. Kaplan, and Ann E. Nelson, “Cosmological implications of dynamical supersymmetry breaking,” *Phys. Rev. D* **49**, 779–787 (1994), [arXiv:hep-ph/9308292](#).
- [28] Lisa Randall, Jakub Scholtz, and James Unwin, “Flooded Dark Matter and S Level Rise,” *JHEP* **03**, 011 (2016), [arXiv:1509.08477 \[hep-ph\]](#).
- [29] Asher Berlin, Dan Hooper, and Gordan Krnjaic, “PeV-Scale Dark Matter as a Thermal Relic of a Decoupled Sector,” *Phys. Lett. B* **760**, 106–111 (2016), [arXiv:1602.08490 \[hep-ph\]](#).
- [30] Nicolás Bernal, Fatemeh Elahi, Carlos Maldonado, and James Unwin, “Ultraviolet Freeze-in and Non-Standard Cosmologies,” *JCAP* **11**, 026 (2019), [arXiv:1909.07992 \[hep-ph\]](#).
- [31] Jared A. Evans, Akshay Ghalsasi, Stefania Gori, Michele Tammara, and Jure Zupan, “Light Dark Matter from Entropy Dilution,” *JHEP* **02**, 151 (2020), [arXiv:1910.06319 \[hep-ph\]](#).
- [32] C. P. Burgess, Richard Easther, Anupam Mazumdar, David F. Mota, and Tuomas Multamaki, “Multiple inflation, cosmic string networks and the string landscape,” *JHEP* **05**, 067 (2005), [arXiv:hep-th/0501125 \[hep-th\]](#).
- [33] Carroll Wainwright and Stefano Profumo, “The Impact of a strongly first-order phase transition on the abundance of thermal relics,” *Phys. Rev. D* **80**, 103517 (2009), [arXiv:0909.1317 \[hep-ph\]](#).
- [34] Hooman Davoudiasl, Dan Hooper, and Samuel D. McDermott, “Inflatable Dark Matter,” *Phys. Rev. Lett.*

- 116**, 031303 (2016), [arXiv:1507.08660 \[hep-ph\]](#).
- [35] Sebastian Hoof and Joerg Jaeckel, “QCD axions and axionlike particles in a two-inflation scenario,” *Phys. Rev. D* **96**, 115016 (2017), [arXiv:1709.01090 \[hep-ph\]](#).
- [36] Moritz Breitbach, Joachim Kopp, Eric Madge, Toby Opferkuch, and Pedro Schwaller, “Dark, Cold, and Noisy: Constraining Secluded Hidden Sectors with Gravitational Waves,” *JCAP* **07**, 007 (2019), [arXiv:1811.11175 \[hep-ph\]](#).
- [37] Thomas Hambye, Alessandro Strumia, and Daniele Teresi, “Super-cool Dark Matter,” *JHEP* **08**, 188 (2018), [arXiv:1805.01473 \[hep-ph\]](#).
- [38] Edward Hardy and Robert Lasenby, “Stellar cooling bounds on new light particles: plasma mixing effects,” *JHEP* **02**, 033 (2017), [arXiv:1611.05852 \[hep-ph\]](#).
- [39] Simon Knapen, Tongyan Lin, and Kathryn M. Zurek, “Light Dark Matter: Models and Constraints,” *Phys. Rev. D* **96**, 115021 (2017), [arXiv:1709.07882 \[hep-ph\]](#).
- [40] Arkady B. Migdal, *Qualitative Methods in Quantum Theory*, Vol. 48 (1977).
- [41] Lev Davidovich Landau and E.M. Lifshits, *Quantum Mechanics: Non-Relativistic Theory*, Course of Theoretical Physics, Vol. v.3 (Butterworth-Heinemann, Oxford, 1991).
- [42] Masahiro Ibe, Wakutaka Nakano, Yutaro Shoji, and Kazumine Suzuki, “Migdal Effect in Dark Matter Direct Detection Experiments,” *JHEP* **03**, 194 (2018), [arXiv:1707.07258 \[hep-ph\]](#).
- [43] Matthew J. Dolan, Felix Kahlhoefer, and Christopher McCabe, “Directly detecting sub-GeV dark matter with electrons from nuclear scattering,” *Phys. Rev. Lett.* **121**, 101801 (2018), [arXiv:1711.09906 \[hep-ph\]](#).
- [44] R. Bernabei *et al.*, “On electromagnetic contributions in WIMP quests,” *Int. J. Mod. Phys. A* **22**, 3155–3168 (2007), [arXiv:0706.1421 \[astro-ph\]](#).
- [45] Ch.C. Moustakidis, J.D. Vergados, and H. Ejiri, “Direct dark matter detection by observing electrons produced in neutralino-nucleus collisions,” *Nucl. Phys. B* **727**, 406–420 (2005), [arXiv:hep-ph/0507123](#).
- [46] H. Ejiri, Ch.C. Moustakidis, and J.D. Vergados, “Dark matter search by exclusive studies of X-rays following WIMPs nuclear interactions,” *Phys. Lett. B* **639**, 218–222 (2006), [arXiv:hep-ph/0510042](#).
- [47] Daniel Baxter, Yonatan Kahn, and Gordan Krnjaic, “Electron Ionization via Dark Matter-Electron Scattering and the Migdal Effect,” *Phys. Rev. D* **101**, 076014 (2020), [arXiv:1908.00012 \[hep-ph\]](#).
- [48] Simon Knapen, Jonathan Kozaczuk, and Tongyan Lin, “The Migdal effect in semiconductors,” (2020), [arXiv:2011.09496 \[hep-ph\]](#).
- [49] Wolfgang Lotz, “Electron-Impact Ionization Cross-Sections and Ionization Rate Coefficients for Atoms and Ions,” *Zeitschrift für Physik* **14**, 207 (1967).
- [50] G. Massacrier, A.Y. Potekhin, and G. Chabrier, “Equation of state for partially ionized carbon and oxygen mixtures at high temperatures,” *Phys. Rev. E* **84**, 056406 (2011), [arXiv:1111.0532 \[physics.plasm-ph\]](#).
- [51] T. Padmanabhan, *Theoretical Astrophysics*, Vol. 1 (Cambridge University Press, 2000).
- [52] Georgeanne R. Caughlan and William A. Fowler, “Thermonuclear reaction rates. 5,” *Atom. Data Nucl. Data Tabl.* **40**, 283–334 (1988).
- [53] A. M. Dziewonski and D. L. Anderson, “Preliminary reference earth model,” *Phys. Earth Planet. Interiors* **25**, 297–356 (1981).
- [54] F.W. Clarke and H.S. Washington, *The Composition of the Earth’s Crust*, Geological Survey professional paper No. nos. 126-127 (U.S. Government Printing Office, 1924).
- [55] Haiyang S. Wang, Charles H. Lineweaver, and Trevor R. Ireland, “The elemental abundances (with uncertainties) of the most earth-like planet,” *Icarus* **299**, 460 – 474 (2018).
- [56] John W. Morgan and Edward Anders, “Chemical composition of earth, venus, and mercury,” *Proceedings of the National Academy of Sciences* **77**, 6973–6977 (1980).
- [57] W.F. McDonough, “2.15 - compositional model for the earth’s core,” in *Treatise on Geochemistry*, edited by Heinrich D. Holland and Karl K. Turekian (Pergamon, Oxford, 2003) pp. 547 – 568.
- [58] David H. Johnston, Thomas R. McGetchin, and M. Nafi Toksöz, “The thermal state and internal structure of mars,” *Journal of Geophysical Research* (1896-1977) **79**, 3959–3971 (1974).
- [59] Joseph Bramante, Benjamin Broerman, Rafael F. Lang, and Nirmal Raj, “Saturated Overburden Scattering and the Multiscatter Frontier: Discovering Dark Matter at the Planck Mass and Beyond,” *Phys. Rev. D* **98**, 083516 (2018), [arXiv:1803.08044 \[hep-ph\]](#).
- [60] M.G. Aartsen *et al.* (IceCube), “The IceCube Neutrino Observatory: Instrumentation and Online Systems,” *JINST* **12**, P03012 (2017), [arXiv:1612.05093 \[astro-ph.IM\]](#).
- [61] G. Bellini *et al.* (Borexino), “Final results of Borexino Phase-I on low energy solar neutrino spectroscopy,” *Phys. Rev. D* **89**, 112007 (2014), [arXiv:1308.0443 \[hep-ex\]](#).
- [62] S. Andringa *et al.* (SNO+), “Current Status and Future Prospects of the SNO+ Experiment,” *Adv. High Energy Phys.* **2016**, 6194250 (2016), [arXiv:1508.05759 \[physics.ins-det\]](#).
- [63] Aniket Joglekar, Nirmal Raj, Philip Tanedo, and Hai-Bo Yu, “Relativistic capture of dark matter by electrons in neutron stars,” *Phys. Lett. B*, 135767 (2020), [arXiv:1911.13293 \[hep-ph\]](#).
- [64] Aniket Joglekar, Nirmal Raj, Philip Tanedo, and Hai-Bo Yu, “Dark kinetic heating of neutron stars from contact interactions with relativistic targets,” *Phys. Rev. D* **102**, 123002 (2020), [arXiv:2004.09539 \[hep-ph\]](#).
- [65] Javier Acevedo, Joseph Bramante, and Alan Goodman, “Accelerating dark matter discovery,” to appear.
- [66] Joseph Bramante, Andrew Buchanan, Alan Goodman, and Eesha Lodhi, “Terrestrial and Martian Heat Flow Limits on Dark Matter,” *Phys. Rev. D* **101**, 043001 (2020), [arXiv:1909.11683 \[hep-ph\]](#).
- [67] Javier F. Acevedo, Joseph Bramante, Alan Goodman, Joachim Kopp, and Toby Opferkuch, “Dark Matter, Destroyer of Worlds: Neutrino, Thermal, and Existential Signatures from Black Holes in the Sun and Earth,” (2020), [arXiv:2012.09176 \[hep-ph\]](#).
- [68] Joseph Bramante, “Dark matter ignition of type Ia supernovae,” *Phys. Rev. Lett.* **115**, 141301 (2015), [arXiv:1505.07464 \[hep-ph\]](#).
- [69] Peter W. Graham, Surjeet Rajendran, and Jaime Varela, “Dark Matter Triggers of Supernovae,” *Phys. Rev. D* **92**, 063007 (2015), [arXiv:1505.04444 \[hep-ph\]](#).
- [70] Peter W. Graham, Ryan Janish, Vijay Narayan, Surjeet Rajendran, and Paul Riggins, “White Dwarfs as Dark Matter Detectors,” *Phys. Rev. D* **98**, 115027 (2018),

- [arXiv:1805.07381 \[hep-ph\]](#).
- [71] Javier F. Acevedo and Joseph Bramante, “Supernovae Sparked By Dark Matter in White Dwarfs,” *Phys. Rev. D* **100**, 043020 (2019), [arXiv:1904.11993 \[hep-ph\]](#).
 - [72] Ryan Janish, Vijay Narayan, and Paul Riggins, “Type Ia supernovae from dark matter core collapse,” *Phys. Rev. D* **100**, 035008 (2019), [arXiv:1905.00395 \[hep-ph\]](#).
 - [73] Michael A. Fedderke, Peter W. Graham, and Surjeet Rajendran, “White dwarf bounds on charged massive particles,” *Phys. Rev. D* **101**, 115021 (2020), [arXiv:1911.08883 \[hep-ph\]](#).
 - [74] F. X. Timmes and S. E. Woosley, “The conductive propagation of nuclear flames. I - Degenerate C + O and O + NE + MG white dwarfs,” *Astrophys. J.* **396**, 649–667 (1992).
 - [75] A.Y. Potekhin, D.A. Baiko, P. Haensel, and D.G. Yakovlev, “Transport properties of degenerate electrons in neutron star envelopes and white dwarf cores,” *Astron. Astrophys.* **346**, 345 (1999), [arXiv:astro-ph/9903127](#).
 - [76] S. L. Shapiro and S. A. Teukolsky, *Black holes, white dwarfs, and neutron stars: The physics of compact objects*. New York, Wiley-Interscience, 1983, 663 p. (1983).
 - [77] L.R. Gasques, A.V. Afanasjev, E.F. Aguilera, M. Beard, L.C. Chamon, P. Ring, M. Wiescher, and D.G. Yakovlev, “Nuclear fusion in dense matter: Reaction rate and carbon burning,” *Phys. Rev. C* **72**, 025806 (2005), [arXiv:astro-ph/0506386](#).
 - [78] Pierre Descouvemont, Abderrahim Adahchour, Carmen Angulo, Alain Coc, and Elisabeth Vangioni-Flam, “Compilation and R-matrix analysis of Big Bang nuclear reaction rates,” *Atom. Data Nucl. Data Tabl.* **88**, 203–236 (2004), [arXiv:astro-ph/0407101](#).
 - [79] S. Ando, R.H. Cyburt, S.W. Hong, and C.H. Hyun, “Radiative neutron capture on a proton at BBN energies,” *Phys. Rev. C* **74**, 025809 (2006), [arXiv:nucl-th/0511074](#).
 - [80] Karsten Jedamzik and Maxim Pospelov, “Big Bang Nucleosynthesis and Particle Dark Matter,” *New J. Phys.* **11**, 105028 (2009), [arXiv:0906.2087 \[hep-ph\]](#).
 - [81] W. Greiner, *Relativistic quantum mechanics: Wave equations* (1990).